journal

J. Am. Ceram. Soc., **88** [7] 1900–1908 (2005)
DOI: 10.1111/j.1551-2916.2005.00412.x

On the Effect of Local Grain-Boundary Chemistry on the Macroscopic Mechanical Properties of a High-Purity Y_2O_3-Al_2O_3-Containing Silicon Nitride Ceramic: Role of Oxygen

A. Ziegler and J. M. McNaney

Materials Science and Technology Division, Lawrence Livermore National Laboratory, Livermore, California 94551

M. J. Hoffmann

Institut für Keramik im Maschinenbau, Universität Karlsruhe, D-76131 Karlsruhe, Germany

R. O. Ritchie[†]

Materials Sciences Division, Lawrence Berkeley National Laboratory, and Department of Materials Science and Engineering, University of California, Berkeley, California 94720

The effects of grain-boundary chemistry on the mechanical properties of high-purity silicon nitride ceramics have been investigated, specifically involving the role of oxygen, present along the grain boundaries, in influencing the fracture behavior. To avoid complications from inadvertently introduced impurities, studies were performed on a high-purity Si_3N_4 processed using two-step gas-pressure-HIP sintering. Varying the grain-boundary oxygen content, which was achieved by control of oxidizing heat treatments and sintering additives, was found to result in a transition in fracture mechanism, from transgranular to intergranular fracture, with an associated increase in fracture toughness. This phenomenon is correlated to an oxygen-induced change in grain-boundary chemistry and possibly to a concomitant structural transformation along the interface. The incorporation of oxygen appears to affect fracture by "weakening" the interface, thus facilitating debonding and crack advance along the boundaries, and hence to toughening by grain bridging. It is concluded that if the oxygen content in the thin grain-boundary films exceeds a lower limit, which is $\sim$0.87 equiv% oxygen content, then the interfacial structure and bonding characteristics favor intergranular debonding during crack propagation; otherwise, transgranular fracture ensues.

I. Introduction

The properties of silicon nitride ceramics are strongly influenced by microstructure and the chemical composition of the grain-boundary phase. Indeed, during processing, the grain boundary is the key microstructural feature that dictates the mechanical properties. It has long been recognized that the room-temperature strength and toughness of monolithic Si_3N_4 ceramic materials depend strongly upon the microstructure and crack path. Generally, fine-grained materials exhibit the highest strength, while high toughness is promoted by large-grained microstructures and an intergranular fracture path. Whereas strength is commonly associated with flaw size, which is invariably related to grain size, toughness is generally attributed to dissipative mechanisms acting behind the crack tip, including grain bridging and frictional pull-out.[1–17] Consequently, a microstructure of fine, elongated grains that fails intergranularly generally provides both high toughness and good strength. The precise reasons why a ceramic fails intergranularly, as opposed to transgranularly, however, are still uncertain, although the predominant view is that by "weakening" the interface, debonding and crack advance along the boundaries are facilitated. Accordingly, interface strength and crack path must be controlled by the chemical composition, atomic structure, and bonding along the grain-boundary phase.

In this work, we examine two highly pure Si_3N_4 ceramics, containing Y_2O_3 and Al_2O_3 as additives, and specifically investigate the change in fracture mechanism and crack path, which is critical to defining the mechanical properties, in terms of the effect of (i) post-sintering heat treatments and (ii) slight variations in grain-boundary composition. Our approach is to focus on the role of *local* grain-boundary chemistry and its relation to crack propagation and *macroscopic* mechanical properties.

II. Background

Grain boundaries in most silicon nitrides have a typical width of 1–5 nm. This equilibrium size is considered to be a function of chemical composition[18–26] rather than the amount of additive; processing parameters, such as sintering temperature, time, and pressure, appear to have little effect. The additives tend to segregate along boundaries and accumulate at the triple junctions.[27–29] Oxygen also accumulates at the boundaries, and is assumed to have a marked effect (possibly more significant than that of other sintering additives) on the mechanical properties.

Post-sintering heat treatments have invariably been found to improve the strength, creep, and toughness properties of Si_3N_4 ceramics[30–38]; sound explanations as to why this happens have been generally inconclusive, in part due to the complexity of the oxidation/devitrification processes that occur during such heat treatments. A partially crystallized boundary phase usually exists at multiple-grain junctions, while the remainder of the liquid sintering aid solidifies as a thin amorphous film between the crystalline phases.[27–30] Thermodynamic considerations of the specific local chemistry and interfacial atomic structure govern the existence of these amorphous films.[39] The devitrification of the grain boundaries and the effects that it has on the mechanical properties have suggested two different explanations for the improvements in strength and toughness.[40–49] The first argues that the structure and bonding characteristics of the thin grain-boundary films are critical in governing the strength and tough-

M. Cinibulk—contributing editor

Manuscript No. 20271. Received June 23, 2004; approved March 7, 2005.
Supported by the Director, Office of Science, Office of Basic Energy Sciences, Division of Materials Sciences and Engineering of the U.S. Department of Energy under Contract No. DE-AC03-76SF00098.
[†]Author to whom correspondence should be addressed. e-mail: RORitchie@LBL.gov

ness of the bulk ceramic.[40–45] As post-sintering heat treatments can alter the local atomic structure and bonding along the thin grain boundaries, this can promote debonding there, leading to intergranular fracture and toughening from grain bridging. An alternative explanation involves the mismatch of thermal expansion coefficients between the crystallized, or partially crystallized, triple points, the thin amorphous grain-boundary films, and the matrix grains.[46–49] As the thermal expansion coefficient of the amorphous grain-boundary film is high compared with that of the adjacent grains, the contraction of the crystalline intergranular material is larger than that of the corresponding amorphous phase, resulting in tensile residual stresses, capable of initiating cracking in, and adjacent to, the boundary, particularly in the vicinity of the partially crystalline triple junctions. It is conceivable that both mechanisms operate *in concert*, with the tensile residual stresses promoting crack initiation and the local bonding promoting crack growth along the boundaries.

During oxidizing heat treatments, oxygen diffuses into the microstructure while sintering aid cations diffuse outward to the surface.[50–53] It has been suggested that oxygen replaces nitrogen at the grain boundary and its interfaces with neighboring matrix grains.[54–57] This would be in agreement with calculated binding energies of Si-tetrahedral clusters with various N:O ratios, showing that the Si–O bond will provide the most reduction in energy and therefore will be more favorable than the Si–N bond.[54] Similarly, with Al–O and Al–N tetrahedral clusters, Al–O will exhibit the stronger bond. The binding energy of SiN_xO_y and AlN_xO_y clusters increases systematically when O substitutes for N. Hence, of the tetrahedral structures, the four structures SiO_4, $SiNO_3$, SiN_2O_2, and AlO_4 are theoretically the most stable.[54] These results are in good agreement with nuclear magnetic resonance studies of Si–Al–Y oxynitride glasses, showing that the glass films are made up of SiO_4, $SiNO_3$, SiN_2O_2, and AlO_4 tetrahedra.[55] Consequently, each oxygen atom added to Si_3N_4, containing among its sintering additives Al_2O_3, would introduce an additional Si–O or Al–O cross bond; as replacements for Si–N, or Al–N-type cross-bonds, they would act to *strengthen* interfacial cohesion. In contrast, studies on the debonding behavior of β-Si_3N_4 whiskers in Si–Al–Y oxynitride glass have shown that a decrease in the N:O ratio *weakens* interfacial cohesion.[45,46]

Such theoretical calculations assume a simplified model of pure Si–O–N glass. The reality is quite different though, as actual grain-boundary phases are (i) composed of more than just Si, O, and N atoms and (ii) they are confined to a few nanometers in width. Moreover, their atomic structure has to connect to differently oriented Si_3N_4 matrix grains on both sides. To date, no investigation has examined the correlation between oxygen content and grain-boundary weakening in a real, dense Si_3N_4 ceramic with typically very thin grain boundaries. This is a major objective of the present study, and is achieved by using heat treatment to vary the oxygen content along the grain boundaries.

III. Experimental Procedures

(1) Materials and Heat Treatment

Conventional densification processing of silicon nitride ceramics generally has used glass encapsulation, resulting in the introduction of impurity elements originating from the glass encapsulation of the green body. To minimize this problem, Si_3N_4 ceramics in the present study were uniquely fabricated without glass encapsulation, resulting in a highly pure material with very controlled amounts of sintering additives. Specifically, fabrication was achieved via a two-step gas pressure sintering and a subsequent hot-isostatic-pressing densification technique.[58] Such high-purity, controlled processing, with impurity-free densification, was utilized to discern the specific role of small quantities of sintering additions. Two different Si_3N_4 compositions were examined, containing Y_2O_3 and Al_2O_3 as sintering additives. The two compositions are designated as (2/0/1) and (2/0/0) by the nominal amount and type of sintering additive ($Y_2O_3/SiO_2/Al_2O_3$), as described in Table I. Although not intentionally added, SiO_2 is an inherent component of the ceramic body as the Si_3N_4 powder particles are covered by a fine SiO_2 layer. The resulting microstructures of both compositions consisted of exclusively β-Si_3N_4 in both acicular-shaped and equiaxed grains (Fig. 1).

In addition to the as-sintered material, a set of samples of the same batch was subjected to a post-sintering heat treatment of varying duration (25, 50, 100, and 200 h) at 1400°C in air. Based on studies of the microstructure and oxide formation, this heat treatment was selected so that both the transition to and the final chemical/microstructural equilibrium state could be examined. The average grain size, determined according to ASTM E112-96, and aspect ratios before and after heat treatment are listed in Table II.

(2) Mechanical Testing

Hardness and fracture toughness properties were measured using indentation techniques, the toughness being evaluated by inducing crack formation under a standard Vickers indenter using 5, 7, 10, 12, and 15 kg loads. Twenty-five indents per sample (five indents per load), resulting in a total of 1050 crack lengths, were measured under an optical microscope, with the hardness, H, and indentation fracture toughness, K_c, calculated using the relationships[5]:

$$H = \frac{P}{2 \times \left(\frac{a}{2}\right)^2} \tag{1}$$

$$K_c = 0.016 \times \left(\frac{E}{H}\right)^{1/2} \times \frac{P}{\left(\frac{c}{2}\right)^{3/2}} \tag{2}$$

where P is the applied load, E is the Young's modulus (taken to be 300 GPa), a is the diagonal of the Vickers indent, and c is the total length of the crack extending from the corners of the indent. By determining the toughness over a range of indentation loads, i.e., over a range of crack sizes, an estimate of the resistance-curve (R-curve) behavior was obtained.

(3) Characterization

Energy-dispersive X-ray emission spectroscopy (EDX) was carried out on thin transmission electron microscopy (TEM) samples in a Philips CM200/FEG TEM (Hillsborough, OR) to discern the distribution of chemical elements along and across the boundaries. With the EDX detector (Oxford Microanalysis 6767, Oxford, UK), spatially resolved compositional analysis ($Z > 5$) could be performed with an energy resolution of 136 eV for Mn$K\alpha$ radiation. The EDX probe diameter could be focused to a 1.2 nm small spot to detect the signal emanating from a 1–5 nm thin grain-boundary film. EDX spectra were collected by (i) line scans across the thin grain boundaries and (ii) spectra covering an area of 20 nm × 20 nm from approximately the center of the triple junctions. On each specimen, five spectra on the grain boundaries and five spectra on the triple points were collected. For the spectra measured on thin grain boundaries, it was necessary to align the grain boundary as edge-on as possible, usually by orienting the grain to one side of it along a low index zone axis, i.e., mostly [0001]. Effects like beam broadening and

Table I. Silicon Nitride Material Compositions Investigated in this Study

	Nominal composition (wt%)				Mol (mol%)			
	Si_3N_4	Y_2O_3	SiO_2	Al_2O_3	Si_3N_4	Y_2O_3	SiO_2	Al_2O_3
(2/0/1)	97.0	2.0	0	1.0	97.4	1.2	0	1.4
(2/0/0)	98.0	2.0	0	0	98.7	1.3	0	0

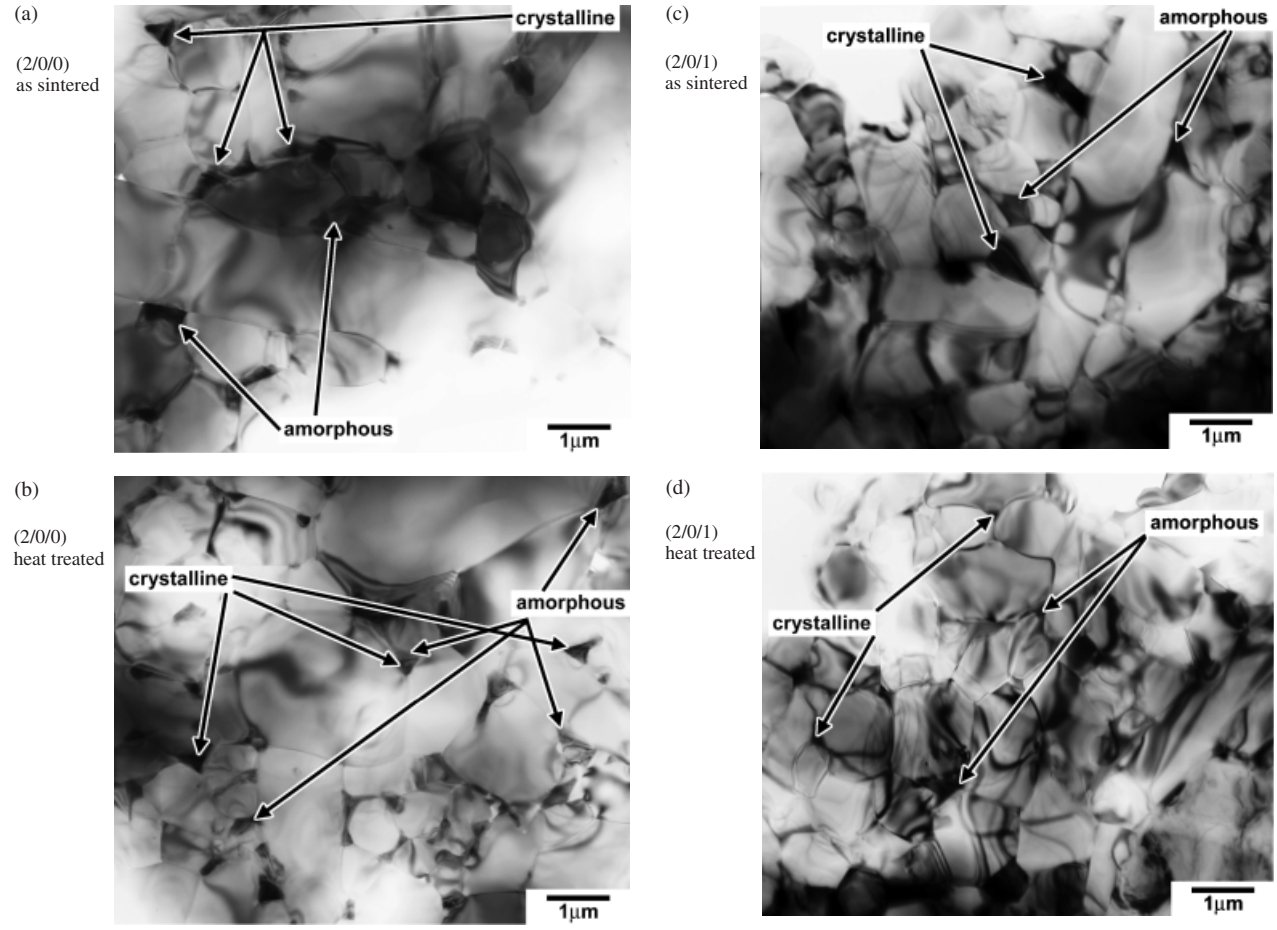

Fig. 1. TEM images of the microstructure of both material compositions in their as-sintered and 200 h heat-treated states, respectively, (a, b) (2/0/0) and (c, d) (2/0/1). The arrows indicate crystalline and amorphous triple points.

sampling depth are negligible when collecting the EDX signal in a TEM, because the TEM specimen thickness is usually much less than the EDX excitation depth and thus, beam broadening is insignificant. The individual EDX spectra were background normalized.

Scanning electron microscopy (SEM) of the fracture surfaces was performed using a JEOL 6300 scanning electron microscope (Tokyo, Japan). SEM was also used to measure the oxide layer thickness after heat-treatment cycles to assess the oxidation behavior. In order to measure this layer thickness, the samples were broken, instead of cut, along the fracture surfaces; contrast differences between the bulk material and the oxide layer helped in measuring the layer thickness.

IV. Results and Discussion

(1) Toughness and Fractography

Except for grain-boundary chemistry, the microstructures of the initial as-sintered (2/0/1) and (2/0/0) compositions differ only in grain size (Fig. 1); whereas the grain aspect ratio is the same, the Al-containing (2/0/1) material exhibits a factor of two smaller grain size than the Al-free (2/0/0) material (Table II). Following the oxidizing heat treatments, the morphology of these microstructures appeared unchanged; there was no additional grain growth, no microstructural coarsening, and no change in aspect ratio (Table II). With respect to the morphology of the triple points, any differences after heat treatment were not considered to be significant; only a few triple points crystallized and many amorphous triple points were still seen, even after 200 h at 1400°C in both (2/0/1) and (2/0/0) compositions (Fig. 1). These images show how the amount of grain-boundary phase is distributed among triple points and thin two-grain grain boundaries; the triple points have a larger capacity than the thin films to encompass this secondary phase.

Table II. Average Grain Sizes and Aspect Ratios

	Average grain size (μm)		Aspect ratio	
Composition	a.s.	h.t.	a.s.	h.t.
(2/0/1)	2	2	8	8.1
(2/0/0)	4.1	3.9	8.3	8.2

a.s., as-sintered; h.t., heat treated.

The effect of oxidation during the 1400°C heat treatments is presented in Fig. 2. The primary purpose was to assess the overall oxidation behavior of the two Si_3N_4 variants and to confirm that their oxidation behavior is comparable to other Si_3N_4 ceramics. The surface oxidation rates at 1400°C, measured as the growth of oxide layer thickness over time, indicate a logarithmic oxidation law, which is consistent with diffusion-controlled oxidation through the growing oxide scale.[59–64] The scale itself consists primarily of amorphous SiO_2, embedded with differently sized, elongated $Y_2Si_2O_7$ crystals, the majority of which are pure crystals although some also contain Al. In Fig. 2, it can also be seen that the growth of the surface oxide layer depends on the grain-boundary chemistry, especially with respect to the presence (or absence) of Al_2O_3. Whereas the Al_2O_3-free (2/0/0) material had only thin oxide scales (<2 μm), the Al_2O_3-containing (2/0/1) samples exhibited a pronounced growth in surface oxide, with a layer thickness up to 8 μm. The diffusion paths in Si_3N_4 are primarily the grain boundaries, since at high temperatures, the thin amorphous intergranular films tend to become viscous and facilitate diffusion. The formation of the

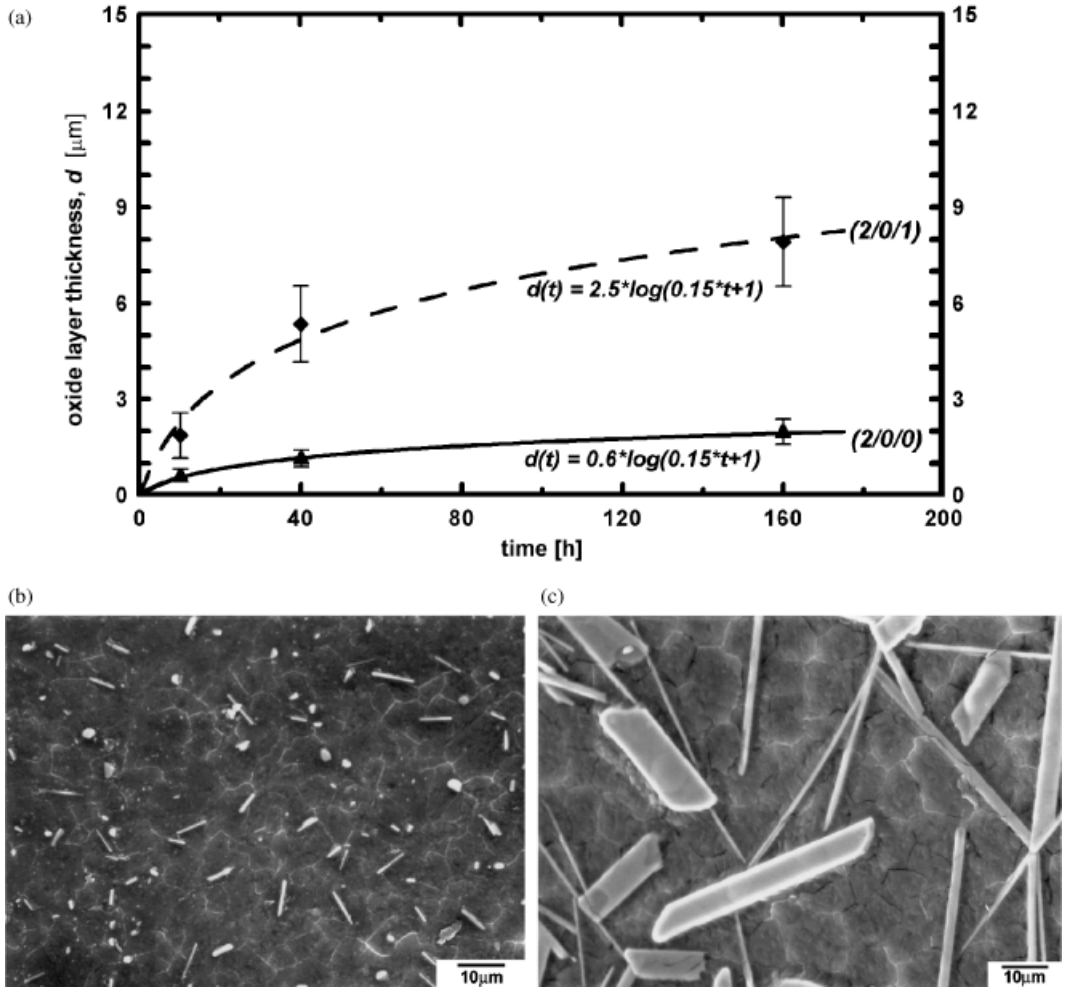

Fig. 2. Oxidation behavior of the material compositions considered in this investigation, showing (a) the growth and thickness of the surface oxide layer and (b) and (c) the formation of the elongated $Y_2Si_2O_7$ surface crystals after (b) 10 h and (c) 160 h on the surface of the (2/0/0) material.

observed surface crystals clearly indicates that Y and Al, and O for that matter, are diffusing along these grain boundaries, which presumably allows for those elements to move to energetically more favorable atomic locations associated with a different chemical bonding state.

The results of the hardness and indentation fracture toughness measurements on both the as-sintered and heat-treated materials are presented in Fig. 3. The hardness (Figs. 3(a),(b)) shows only a marginal decline with increasing indentation load (and hence crack length). Usually at low loads, indentation cracking occurs during unloading; at high loads, however, cracking can occur prematurely during loading, leading to larger indents and hence lower apparent hardness. The results show that the overall effect of grain-boundary chemistry and heat treatment on hardness is minimal for the different Si_3N_4 materials examined.

In contrast, the toughness is significantly affected by grain-boundary chemistry (Figs. 3(c),(d)). In the as-sintered state, the (2/0/1) material clearly shows stable initial crack growth, in that the fracture toughness increases with crack length in the form of rising *R*-curve behavior. Conversely, the (2/0/0) material shows no evidence of such behavior, with unstable fracture occurring immediately at crack initiation. However, with heat treatment, these marked differences gradually disappear, as the (2/0/0) material undergoes a marked change in fracture behavior that completely changes the shape of its *R*-curve and results in an $\sim$180% increase in toughness compared with its as-sintered value. Indeed, after 200 h at 1400°C, the (2/0/0) material exhibits rising *R*-curve behavior and a fracture toughness comparable to that of the (2/0/1) material. In contrast, the evolution of the (2/0/1) material with heat treatment is less dramatic, with only a maximum $\sim$15% increase in toughness and no change in shape of the *R*-curve.

Fractography of the indented and subsequently fractured samples is presented in Figs. 4 and 5. They reveal that the as-sintered (2/0/0) material exhibits a brittle transgranular fracture surface, with no features of grain pull-out and interlocking grains that are typical of many toughened ceramic materials. After heat treatment though, the (2/0/0) composition shows a distinct change in fracture mode, from largely transgranular to largely intergranular. In contrast, fracture in the (2/0/1) material remains predominantly intergranular before and after heat treatment. The intergranular crack paths are consistent with toughening in the crack wake via crack bridging from interlocking grains that act to shield the crack tip from the applied far-field load.[1–3,6–16] Since the bridging is a function of crack size, this is also consistent with the observed *R*-curve behavior in Figs. 3(c) and (d), where the materials display increasing toughness with increasing crack length.

The relatively high toughness of the heat-treated (2/0/0) material, particularly at large crack lengths, can be associated with its larger grain size, as compared with the (2/0/1) material; provided fracture occurs intergranularly, coarse-grained microstructures (with high aspect-ratio grains) are more effective in promoting crack bridging, which acts to inhibit crack extension.[3,6–10] In the as-sintered state, however, such grain-size arguments do not apply as the (2/0/0) material fails transgranularly and hence cannot develop any crack-tip shielding from crack bridging; under these circumstances, the toughness remains low with no rising *R*-curve behavior. Thus, irrespective of microstructural parameters such as grain size and aspect ratio, crack-bridging mechanisms in monolithic ceramics can only be

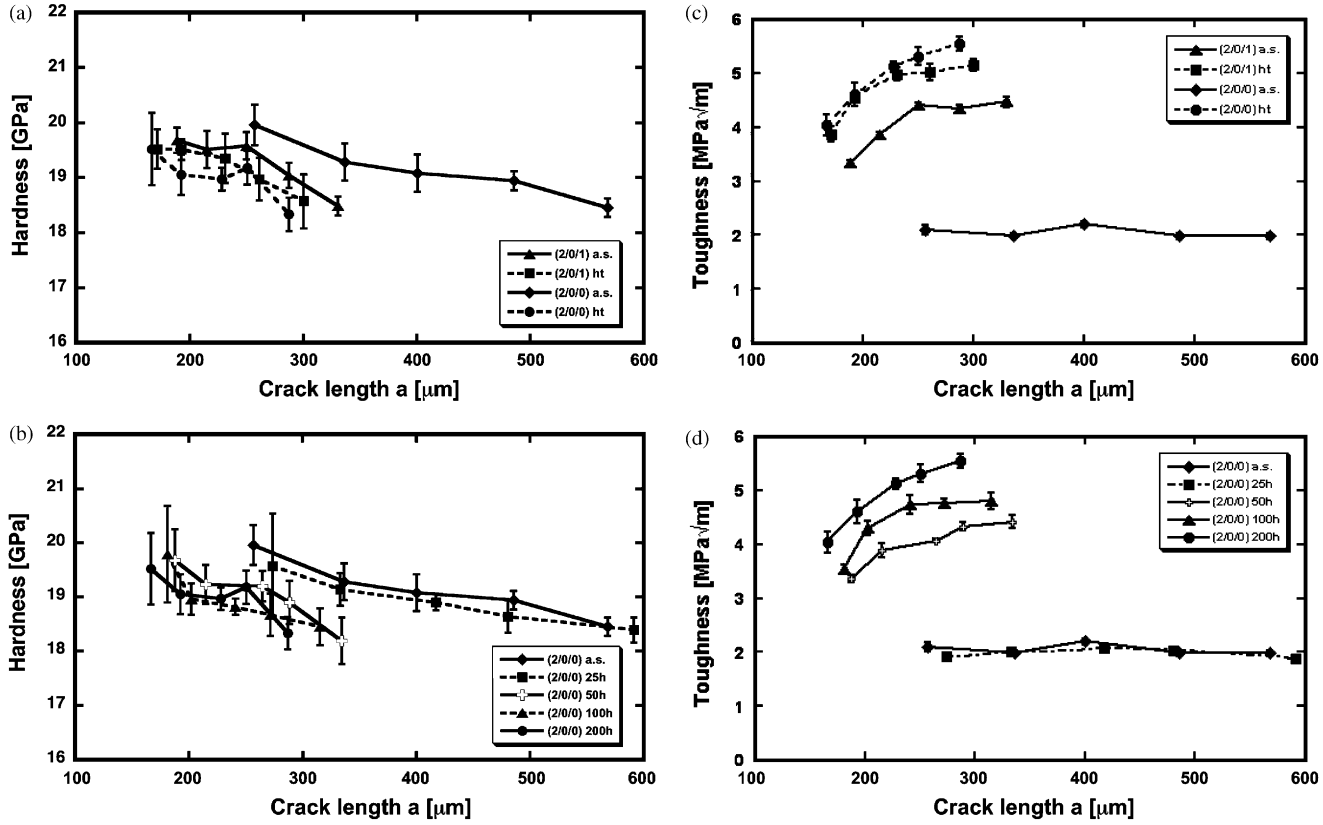

Fig. 3. (a, b) Hardness and (c, d) indentation fracture toughness values for both material compositions in their as-sintered and the heat-treated states.

active if the crack path is intergranular. The nature of the crack path is therefore a central issue, which depends strongly on how the grain-boundary chemistry determines the debonding characteristics.

Whereas the strength, toughness, and fractographic data for the (2/0/0) and (2/0/1) materials are in general agreement with existing notions[3] concerning the toughening of silicon nitrides, it remains to be understood exactly how grain-boundary chemis-

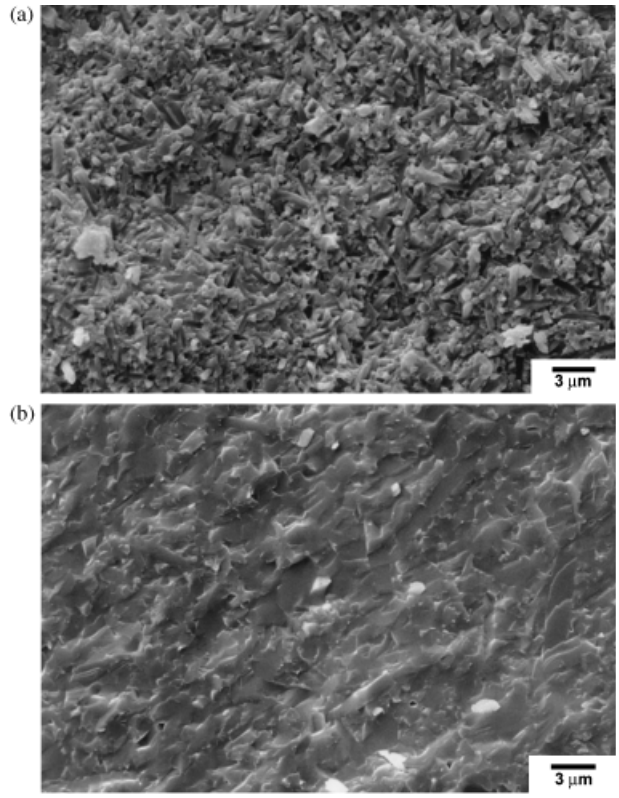

Fig. 4. Fracture surfaces of the as-sintered material compositions (a) (2/0/1) and (b) (2/0/0).

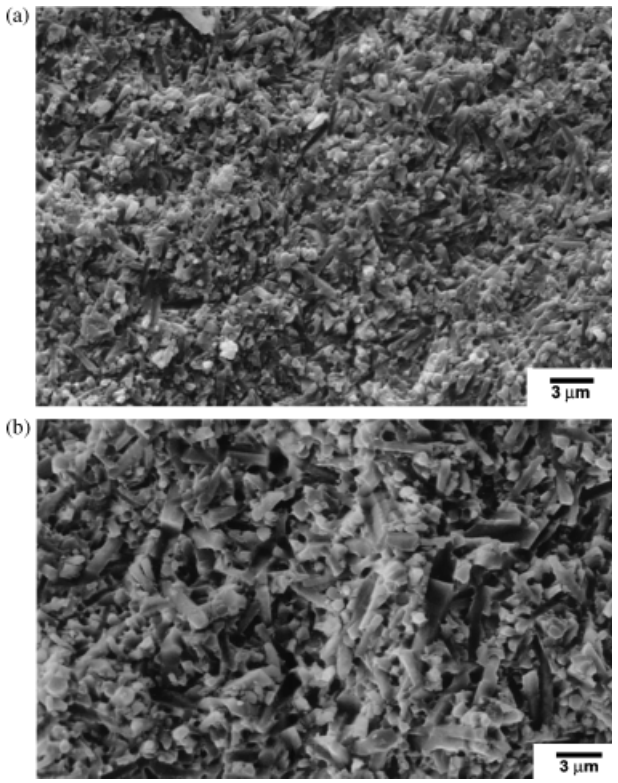

Fig. 5. Fracture surfaces of the heat-treated material compositions (a) (2/0/1) and (b) (2/0/0).

try can affect the choice of crack path. As noted above, in the present work, the use of very high-purity ceramics permits a more rigorous assessment of the chemical and structural factors governing this choice. Of particular interest are how the additives and heat treatment affect the grain-boundary chemistry, bonding, and structure, especially where there were no associated changes in grain size and shape. Two effects are worthy of consideration using detailed grain-boundary characterization:

(1) First, as the grain size and shape remain unchanged, it is clear that the marked increase in toughness and associated rising *R*-curve behavior of the (2/0/0) material after heat treatment follows from the fracture-path transition to intergranular fracture caused by a change in the local atomic structure and bonding characteristics along the boundary that promotes interfacial debonding. We presume here that the 1400°C heat treatment causes a rearrangement and relocation of specific atoms (sintering additives and oxidation products) along grain boundaries.

(2) Second, comparison of the as-sintered (2/0/1) and (2/0/0) materials is interesting as both contain the same amount of yttrium and yet differ by 1 wt% Al_2O_3, which is sufficient to cause a difference in fracture mode. With the addition of Al_2O_3, it is important to note that oxygen, as well as aluminum, may be inherently incorporated into the grain boundary.

(2) Grain-Boundary Analysis

Our hypothesis is that the observed change in fracture mechanism is associated with structural transformations in the grain-boundary phase that incorporate O, N, and the sintering-additive cations, or with the relocation of these ions. With the heat-treated materials, it can be assumed that O is the major element that diffuses inward while Y, Al, and N diffuse outward. Here, changes in the chemical balance and atom rearrangement are expected to only occur locally as the diffusion distances along the boundaries for these elements at 1400°C are only a few hundred micrometers. Consequently, since the possible variation in bonding is limited, we can assume that relocation of elements is more important than the inward or outward diffusion from the entire sample.

Our focus is on the short-range relocation of oxygen, yttrium, and aluminum, using EDX to analyze the elemental composition of the thin grain boundaries as they evolve during the heat treatment. In principle, the grain boundary is assumed to experience a critical structural transformation that markedly changes the bonding characteristics, allowing for either debonding or reinforcement of existing chemical bonds across the interface, which in turn determines the crack path—intergranular or transgranular.

The results of the EDX line scans across the thin grain boundaries are presented in Fig. 6. A single line scan immediately reveals the presence of yttrium segregated along the grain boundaries. Y, Al, and O could be measured as they are not encountered in the matrix and segregate entirely to the boundaries. In contrast, quantitative detection of Si and N levels across the grain boundaries could not be achieved as they are encountered in both the matrix and boundaries, and the strong Si and N signals from the matrix grains marred any slight changes in the thin grain boundaries (Fig. 6(a)).

Using the line scans performed on each specimen, the evolution of the grain-boundary chemical composition (Y, Al, and O) was monitored and is depicted in Figs. 6(b) and (c). To obtain this trend line, the spectra were background normalized and the area under each Y, Al, and O peak (not their peak height) was respectively measured for each heat-treatment stage. Each point on the trend line represents the average of five spectra per specimen. It is apparent from these results that in the Al-free material (2/0/0), yttrium tends to diffuse away from the thin grain boundaries as the heat treatment progresses, while the amount of oxygen increases between the grains; however, a considerable amount of yttrium remains along the thin boundaries. In the Al-containing material (2/0/1), similar observations can be made in that the amount of oxygen increases along the thin grain boundaries, while the corresponding amounts of Y and Al decrease; however, the rate of decrease in Al is slower than with Y.

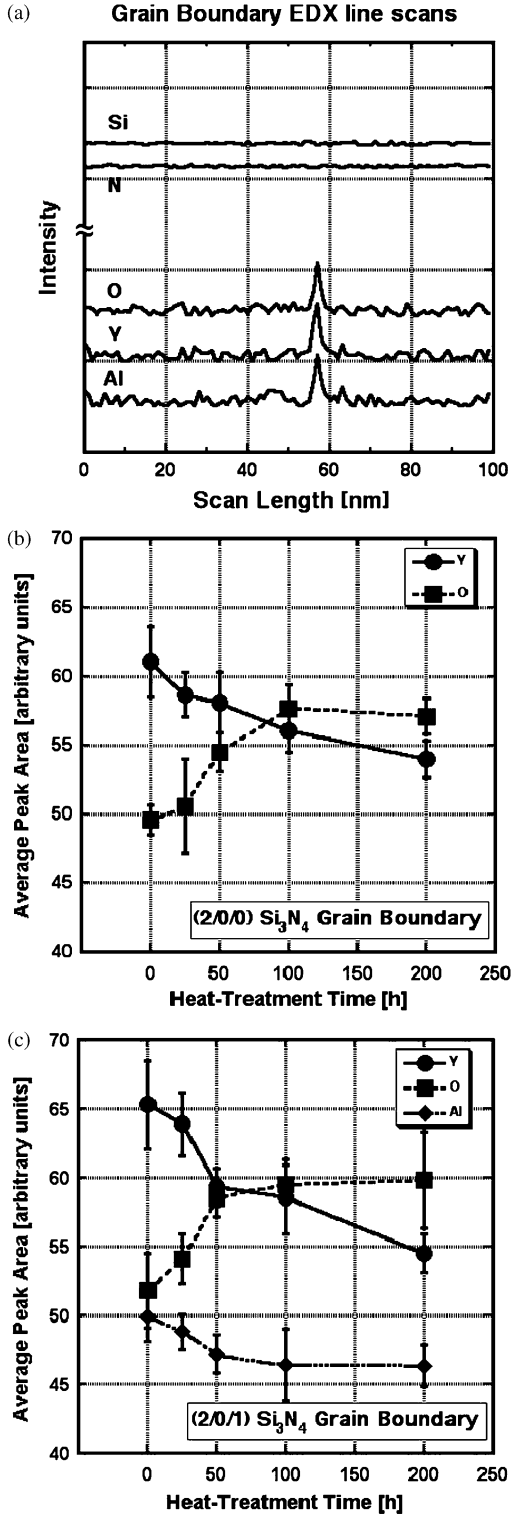

Fig. 6. (a) Example of an EDS line scan spectra revealing the detection of Y, O, and Al along the thin grain boundaries in a (2/0/1) specimen. Note that the intensity axis is not to scale. (b) and (c) show how the grain-boundary chemistry changes during heat treatment.

The corresponding EDX trend lines obtained for the amorphous and crystalline triple points are shown in Figs. 7(a–d). The crystallized triple points examined in the as-sintered material were clearly formed during sintering. Only a few additional triple points crystallized during heat treatment (Fig. 1), leaving most in their amorphous state and allowing EDX analysis of both triple-point morphologies throughout the entire heat-treat-

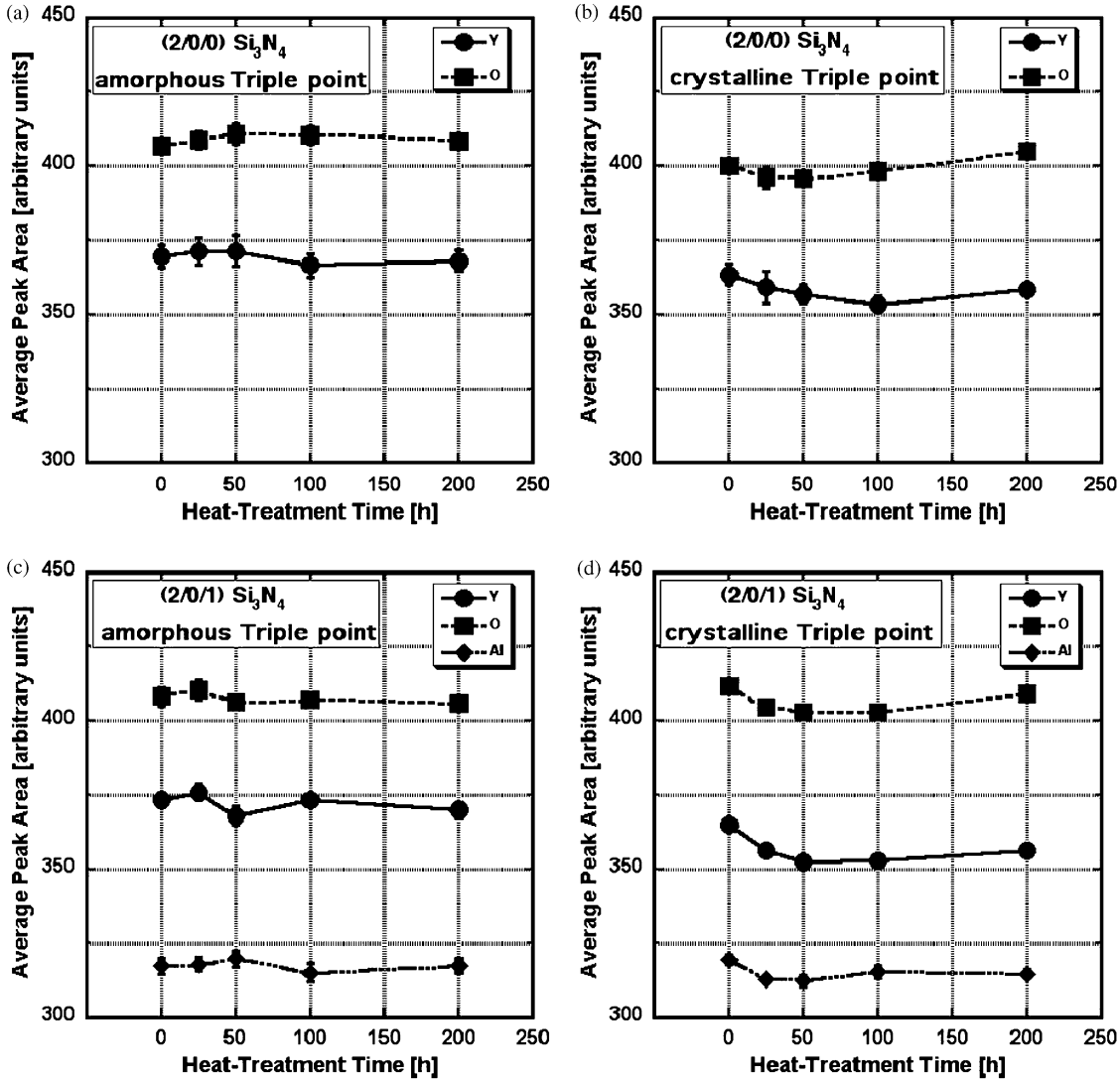

Fig. 7. EDS areal spectra of the triple points showing how the triple-point chemistry changes during heat treatment in the (a,b) (2/0/0) and (c,d) (2/0/1) material.

ment cycle. As seen in Fig. 7, both types of triple points show only marginal changes in their chemical composition during heat treatment. This is because they are regions that are much larger than the thin grain boundaries and therefore contain more grain-boundary phase (segregated chemical elements); as their EDX signal intensity is much stronger than the one emanating from the boundaries, small changes in the triple-point EDX signal intensity are more difficult to discern. The notion that the triple points and the thin grain boundaries are interconnected and thus their respective transformations and chemical balances influence each other can therefore only be examined by analyzing the changes in chemistry in the thin grain boundaries. This result, together with our observations of limited crystallization of the triple points, implies: (i) relative to the thin grain boundaries, the triple points can be regarded as reservoirs of grain-boundary phase and as a sink/source for O, N, Y, and Al cations, and (ii) for the present microstructures, the effects of triple-point crystallization on the mechanical properties are relatively unimportant.

The changes in the chemical balance and atom rearrangement that determine the fracture mode appear to occur at a very local level in the thin amorphous grain boundaries. How explicitly this modification and structural transformation occurs is the focus of continuing investigation. Similarly, it is important to know how the presence/absence of Al and Y cations affects the mechanical properties. It is known, however, that by increasing the amount of oxide-based sintering additives in this same material, i.e., 3, 5, and 7 wt% Y_2O_3, fracture occurs intergranularly.[65] However, it is thought that the incorporation of oxygen into the grain-boundary structure is the primary factor to consider for a structural transformation that markedly changes the bonding and fracture characteristics. Since the observed change in fracture mode occurred as a consequence of the heat treatment, it can be concluded that oxygen is the governing element that affects fracture behavior in the (2/0/0) Si_3N_4 material.

Such results are consistent with theoretical studies of the structure and bonding at grain boundaries in Si_3N_4 ceramics.[66–72] Some of these calculations realistically focus on the incorporation of O into the grain-boundary phase, in keeping with observations that most, if not all, of these thin grain boundaries are found to contain oxygen. It is likely that the Si–N bonds are replaced by Si-O bonds and oxygen takes up the atom positions of nitrogen along the interface. The consequences of this substitution are clear. Experimental results collected in the present work, and in previous studies,[45,46] demonstrate that incorporation of more oxygen into the grain-boundary structure appears to facilitate intergranular debonding. The immediate question here, though, is whether there is a limit in grain-boundary oxygen content that determines whether the ceramic fractures transgranularly or intergranularly.

Table III lists estimated values for the overall oxygen and nitrogen content (in equiv%) and their ratios in both as-sintered (2/0/0) and (2/0/1) materials, obtained from the initial stoic-

Table III. Ratios of Elements in the Si_3N_4 Ceramics Studied

	O/(Si+N+Y+O+(Al)) (eq%)	N/(Si+N+Y+O+(Al)) (eq%)
(2/0/0)	2.406	55.03
(2/0/1)	3.002	54.45

Table IV. Statistical Microstructural Parameters

	Relative area TP/GB	GB EDX signal (areal cps)	Increase in GB EDX signal (%)	GB oxygen content (eq%)
(2/0/0)				
a.s	3.08	49.6	—	0.79
25 h	2.93	50.6	2.02	0.81
50 h	3.03	54.5	9.88	0.87
100 h	3.16	57.7	16.33	0.92
200 h	3.01	57.1	15.12	0.91
	3.04 ± 0.08			
(2/0/1)				
a.s.	2.86	51.8	—	1.04
25 h	2.84	54.1	4.44	1.09
50 h	2.91	58.5	12.93	1.17
100 h	2.97	59.5	14.86	1.19
200 h	2.90	59.8	15.44	1.20
	2.89 ± 0.05			

TP, triple point; GB, grain boundary; EDX, energy-dispersive X-ray emission spectroscopy; a.s., as-sintered.

hiometry when mixing the ceramic powders. These numbers cannot be taken as representative values for the oxygen content along the thin grain boundaries because the grain-boundary phase is also present at the triple points. Also, the oxygen content in the heat-treated samples cannot be quantitatively assessed because it is not known how much oxygen is actually absorbed by the grain boundaries during such heat treatment.

However, a qualitative analysis of the distribution of grain-boundary phase and consequently oxygen among triple points and thin grain boundaries can be performed. A critical assumption is that O is located only in, and is homogeneously distributed along, the grain-boundary phase, i.e., there is no clustering or preferential accumulation, for example, at triple points. To determine the relative volume of triple point versus thin grain boundary, the areas covered by the triple points and by the boundaries were estimated from low-magnification images of the microstructure.[‡] Three TEM images of each of the four microstructures studied were taken; results are listed in Table IV. It can be seen that the volume ratio of triple points to thin grain boundaries is approximately three. Thus, the overall oxygen content listed in Table III needs to be divided accordingly, leaving, for example, 0.79 equiv% of oxygen along thin grain boundaries in the as-sintered (2/0/0) material. Combining this relative content with the corresponding increase in EDX signals measured on the thin grain boundaries can yield estimates of how much oxygen is located in the thin films. These are listed in Table IV where it can be seen that after 50 h at 1400°C, the EDX signal for the (2/0/0) material has increased by 9.88% and the oxygen content along the thin films has increased to 0.87 equiv%. Although this is just a small increase, it is apparent that it is sufficient to locally change the bonding characteristics to such a degree that it causes a fracture mode transition and thereby affects the macroscopic fracture behavior.

The results in Table IV can also be used to estimate the limiting local oxygen content (or otherwise a limit for the nitrogen or a limiting N:O ratio) along the thin grain boundaries that influences the interfacial bond strength and thus affects the fracture-mode change from transgranular to intergranular, which in turn affects the mechanical properties. In the (2/0/0) material, this limit is reached after 50 h at 1400°C when the material first displays rising *R*-curve behavior and intergranular fracture, i.e., at 0.87 equiv% oxygen. The (2/0/1) composition does not experience this change in fracture mode because its thin grain-boundary oxygen content is already above this critical limit in the as-sintered condition.

[‡]This can only be considered as an estimate as measurements are made from two-dimensional images of a three-dimensional microstructure.

V. Conclusions

In an attempt to identify relationships between local grain-boundary composition and macroscopic mechanical behavior, the present study has examined the effects of grain-boundary chemistry on the mechanical properties of two highly pure silicon nitride ceramics, containing, respectively, 2 wt% Y_2O_3 and 2 wt% Y_2O_3/1 wt% Al_2O_3, where the grain-boundary oxygen content could be varied by the amount of sintering additives and by allowing oxygen diffusion from triple points into the grain boundaries during a post-sintering heat treatment. These Si_3N_4 systems were selected because differences in macroscopic fracture behavior are primarily controlled by the grain-boundary oxygen content, rather than microstructural variations such as grain size and shape and crystallization of the triple points; moreover, the presence of intergranular, as opposed to transgranular, fracture is invariably a prerequisite for good fracture properties.

The local oxygen content along the thin grain boundaries was increased by diffusion from triple points during a post-sintering heat treatment at 1400°C. In the Al-free material, this resulted in a change in fracture mode from transgranular to intergranular with a concomitant improvement in mechanical properties; with no change in strength, the material displayed rising *R*-curve behavior with a dramatic increase in fracture toughness by ~180% (after 200 h at 1400°C). [In Si_3N_4 ceramics, intergranular fracture is known to promote interlocking grains in the crack wake, which can enhance the (*R*-curve) toughness through a mechanism of crack bridging].

Such a marked change in mechanical properties was found to be associated with the incorporation of oxygen into the grain boundaries, where its role was to suitably "weaken" the interface, thereby facilitating debonding and intergranular crack advance. EDX analysis of the thin grain boundaries and the triple points revealed qualitative changes in grain-boundary chemistry, specifically the increase in oxygen content and decrease in yttrium and aluminum content during the 1400°C heat treatment. The assumption that there is a grain-boundary oxygen-content limit determining the change in fracture mode could be confirmed. It is concluded that if the incorporation of oxygen into the grain-boundary phase exceeds this (lower) limit, then the interfacial structure and bonding characteristics change in favor of intergranular debonding during crack propagation; otherwise, transgranular fracture occurs. By comparing the changes in fracture mode with the changes in grain-boundary oxygen content, this limit was estimated to be ~0.87 equiv% oxygen.

References

[1]S. M. Wiederhorn, "Brittle Fracture and Toughening Mechanism in Ceramics," *Annu. Rev. Mater. Sci.*, **14**, 373–403 (1984).

[2]R. O. Ritchie, "Mechanisms of Fatigue Crack Propagation in Metals, Ceramics and Composites: Role of Crack Tip Shielding," *Mater. Sci. Eng.*, **A103** [1] 15–28 (1988).

[3]P. F. Becher, "Microstructural Design of Toughened Ceramics," *J. Am. Ceram. Soc.*, **74** [2] 255–69 (1991).

[4]D. R. Clarke, "The Intergranular Film in Silicon Nitride Ceramics: A Diffuse Interface Approach"; pp. 291–301 in *Tailoring of Mechanical Properties of Si_3N_4 Ceramics, NATO ASI Series*, Edited by M. J. Hoffmann and G. Petzow. Kluwer Academic Publishers, Dordrecht, 1994.

[5]B. R. Lawn, *Fracture of Brittle Solids*, 2nd edition, Ch. 8, Cambridge University Press, Cambridge, U.K., 1993.

[6]P. L. Swanson, C. J. Fairbanks, B. R. Lawn, Y.-W. Mai, and B. J. Hockey, "Crack–Interface Grain Bridging as a Fracture Resistance Mechanism in Ceramics: I, Experimental Study on Alumina," *J. Am. Ceram. Soc.*, **70** [4] 279–89 (1987).

[7]Y.-W. Mai and B. R. Lawn, "Crack–Interface Grain Bridging as a Fracture Resistance Mechanism in Ceramics: II, Theoretical Fracture Mechanics Model," *J. Am. Ceram. Soc.*, **70** [4] 289–94 (1987).

[8]J. Rödel, J. F. Kelly, and B. R. Lawn, "In Situ Measurements of Bridged Crack Interfaces in the Scanning Electron Microscope," *J. Am. Ceram. Soc.*, **73** [11] 3313–8 (1990).

[9]Y. Maniette, M. Inagaki, and M. Sakai, "Fracture Toughness and Crack Bridging of a Silicon Nitride Ceramic," *J. Eur. Ceram. Soc.*, **7**, 255–63 (1991).

[10]S. J. Bennison and B. R. Lawn, "Role of Interfacial Grain-Bridging Sliding Friction in Crack Resistance and Strength Properties of Non-Transforming Ceramics," *Acta Metall. Mater.*, **37** [10] 2659–71 (1989).

[11]C.-W. Li and J. Yamanis, "Super-Tough Silicon Nitride with R-Curve Behavior," *Ceram. Eng. Sci. Proc.*, **10** [7–8] 632–45 (1989).

[12]C.-W. Li, D.-J. Lee, and S.-C. Lui, "R-Curve Behavior and Strength for In-Situ-Reinforced Silicon Nitrides with Different Microstructures," *J. Am. Ceram. Soc.*, **75** [7] 1777–85 (1992).

[13]G. Vekinis, M. F. Ashby, and W. R. Beaumont, "R-Curve Behavior of Al_2O_3 Ceramics," *Acta Metall. Mater.*, **38** [6] 1151–62 (1990).

[14]A. Reichl and R. W. Steinbrech, "Determination of Crack-Bridging Forces in Alumina," *J. Am. Ceram. Soc.*, **71** [6] C299–301 (1988).

[15]P. F. Becher, "Crack Bridging Processes in Toughened Ceramics"; pp. 19–33 in *Toughening Mechanisms in Quasi-Brittle Materials*, Edited by S. P. Shah. Kluwer Academic Publishers, Dordrecht, 1991.

[16]R. W. Steinbrech, A. Reichl, and W. Schaarwachter, "R-Curve Behavior of Long Cracks in Alumina," *J. Am. Ceram. Soc.*, **73** [7] 2009–15 (1990).

[17]R. H. Dauskardt, "A Frictional-Wear Mechanism for Fatigue-Crack Growth in Grain Bridging Ceramics," *Acta Metall. Mater.*, **41** [9] 2765–81 (1993).

[18]D. R. Clarke, "On the Equlibrium Thickness of Intergranular Glass Phases in Ceramic Materials," *J. Am. Ceram. Soc.*, **70** [1] 15–22 (1987).

[19]H. J. Kleebe, J. Bruley, and M. Rühle, "HREM and AEM Studies of Yb_2O_3-Fluxed Silicon Nitride Ceramics with and without CaO Addition," *J. Eur. Ceram. Soc.*, **14**, 1–11 (1994).

[20]H. Gu, X. Pan, R. M. Cannon, and M. Rühle, "Dopant Distribution in Grain-Boundary Films in Calcia-Doped Silicon Nitride Ceramics," *J. Am. Ceram. Soc.*, **81** [12] 3125–35 (1998).

[21]H. J. Kleebe, M. K. Cinibulk, R. M. Cannon, and M. Rühle, "Statistical Analysis of the Intergranular Film Thickness in Silicon Nitride Ceramics," *J. Am. Ceram. Soc.*, **76** [8] 1969–77 (1993).

[22]D. R. Clarke, T. M. Shaw, A. P. Philipse, and R. G. Horn, "Possible Electrical Double-Layer Contribution to the Equilibrium Thickness of Intergranular Glass Films in Polycrystalline Ceramics," *J. Am. Ceram. Soc.*, **76** [5] 1201–4 (1993).

[23]H. J. Kleebe, M. J. Hoffmann, and M. Rühle, "Influence of Secondary Phase Chemistry on Grain Boundary Film Thickness in Silicon Nitride," *Z. Metallkd.*, **83** [8] 610–7 (1992).

[24]I. Tanaka, H. J. Kleebe, M. K. Cinibulk, J. Bruley, D. R. Clarke, and M. Rühle, "Calcium Concentration Dependence of the Intergranular Film Thickness in Silicon Nitride," *J. Am. Ceram. Soc.*, **77** [4] 911–4 (1994).

[25]X. Pan, H. Gu, R. van Weeren, S. C. Danforth, R. M. Cannon, and M. Rühle, "Grain Boundary Microstructure and Chemistry of a Hot Isostatically Pressed High-Purity Silicon Nitride," *J. Am. Ceram. Soc.*, **79** [9] 2313–20 (1996).

[26]C. M. Wang, X. Pan, M. J. Hoffmann, R. M. Cannon, and M. Rühle, "Grain Boundary Films in Rare-Earth-Glass-Based Silicon Nitride," *J. Am. Ceram. Soc.*, **79** [3] 788–92 (1996).

[27]M. K. Cinibulk, G. Thomas, and S. M. Johnson, "Fabrication and Secondary-Phase Crystallization of Rare-Earth Disilicate–Silicon Nitride Ceramics," *J. Am. Ceram. Soc.*, **75** [8] 2037–43 (1992).

[28]D. R. Clarke, N. J. Zaluzec, and R. W. Carpenter, "The Intergranular Phase in Hot-Pressed Silicon Nitride: I Elemental Composition," *J. Am. Ceram. Soc.*, **64** [10] 601–7 (1981).

[29]D. R. Clarke, N. J. Zaluzec, and R. W. Carpenter, "The Intergranular Phase in Hot-Pressed Silicon Nitride: II Evidence for Phase Separation and Crystallization," *J. Am. Ceram. Soc.*, **64** [10] 608–11 (1981).

[30]M. K. Cinibulk, G. Thomas, and S. M. Johnson, "Grain-Boundary-Phase Crystallization and Strength of Silicon Nitride Sintered with a YSiAlON Glass," *J. Am. Ceram. Soc.*, **73** [6] 1606–12 (1990).

[31]D. A. Bonnell, T. Y. Tien, and M. Rühle, "Controlled Crystallization of the Amorphous Phase in Silicon Nitride Ceramics," *J. Am. Ceram. Soc.*, **70** [7] 460–5 (1987).

[32]C. T. Bodur, D. V. Szabo, and K. Kromp, "Effects of Heat Treatments on the Microstructure of a Yttria/Alumina Doped Hot Pressed Si_3N_4 Ceramic," *J. Mater. Sci.*, **28**, 2089–96 (1993).

[33]M. K. Cinibulk and H. J. Kleebe, "Effects of Oxidation on Intergranular Phases in Silicon Nitride Ceramics," *J. Mater. Sci.*, **28**, 5775–82 (1993).

[34]F. F. Lange, B. I. Davis, and H. C. Graham, "Compressive Creep and Oxidation Resistance of an Si_3N_4 Material Fabricated in the System Si_3N_4–Si_2N_2O–$Y_2Si_2O_7$," *J. Am. Ceram. Soc.*, **66** [6] C98–9 (1983).

[35]F. F. Lange, B. I. Davis, and M. G. Metcalf, "Strengthening of Polyphase Si_3N_4 Materials trough Oxidation," *J. Mater. Sci.*, **18**, 1497–505 (1983).

[36]M. Ohashi, S. Kanzaki, and H. Tabata, "Processing, Mechanical Properties, and Oxidation Behavior of Silicon Oxynitride Ceramics," *J. Am. Ceram. Soc.*, **74** [1] 109–14 (1991).

[37]H. Klemm and G. Pezzotti, "Fracture Toughness and Time-Dependent Strength Behavior of Low-Doped Silicon Nitrides for Applications at 1400°C," *J. Am. Ceram. Soc.*, **77** [2] 553–61 (1994).

[38]N. L. Hecht, M. G. Steven, L. Chuck, D. E. McCullum, and V. J. Tennery, "Mechanical Properties Characterization of One SiC and Two Si_3N_4 Commercially Available Ceramics," *Ceram. Bull.*, **71** [4] 653–9 (1992).

[39]H. D. Ackler and Y. M. Chiang, "Model Experiment on Thermodynamic Stability of Retained Intergranular Amorphous Films," *J. Am. Ceram. Soc.*, **80** [7] 1893–96 (1997).

[40]E. Y. Sun, P. F. Becher, S. B. Waters, C-H. Hsueh, K. P. Plucknett, and M. J. Hoffmann, "Control of Interface Fracture in Silicon Nitride Ceramics: Influence of Different Rare Earth Elements"; pp. 779–86 in *Ceramic Microstructure: Control at the Atomic Level*, Edited by A. P. Tomsia and A. Glaeser. Plenum Press, New York, 1998.

[41]P. F. Becher, E. Y. Sun, C. H. Hsueh, K. B. Alexander, S. L. Hwang, S. B. Waters, and C. G. Westmoreland, "Debonding of Interfaces Between Beta-Silicon Nitride Whiskers and Si–Al–Y Oxynitride Glasses," *Acta Mater.*, **44** [10] 3881–93 (1996).

[42]E. Y. Sun, K. B. Alexander, P. F. Becher, and S. L. Hwang, "β-Si_3N_4 Whiskers Embedded in Oxynitride Glasses: Interfacial Microstructure," *J. Am. Ceram. Soc.*, **79** [10] 2626–32 (1996).

[43]Y. Tajima, K. Urashima, M. Watanabe, and Y. Matsuo, "Fracture Toughness and Microstructure Evaluation of Silicon Nitride Ceramics"; pp. 167–74 in *Ceramic Transactions*, Vol. 1. Edited by E. R. Fuller and H. Hausner. American Ceramic Society, Westerville, OH, 1988.

[44]Y. Tajima, "Development of High Performance Silicon Nitride Ceramics and their Applications"; pp. 219–24 in *Materials Research Society Proceedings*, Vol. 287. Edited by I. W. Chen, P. F. Becher, M. Mitomo, G. Petzow, and T. S. Yen. Materials Research Society, Boston, MA, 1993.

[45]G. Wotting and G. Ziegler, "Influence of Powder Properties and Processing Conditions on Microstructure and Mechanical Properties of Sintered Si_3N_4," *Ceram. Int.*, **10** [1] 18–22 (1984).

[46]R. Raj and F. F. Lange, "Crystallization of Small Quantities of Glass (or a Liquid) Segregated in Grain Boundaries," *Acta Metall.*, **29**, 1993–2000 (1981).

[47]W. Pompe and H. Kessler, "Internal Stresses in Silicon Nitride and their Influence on Mechanical Behavior"; pp. 353–64 in *Tailoring of Mechanical Properties of Si_3N_4 Ceramics*, Edited by M. J. Hoffmann and G. Petzow. Kluwer Academic Publishers, Dordrecht, 1994.

[48]I. M. Peterson and T-Y. Tien, "Effect of the Grain Boundary Thermal Expansion Coefficient on the Fracture Toughness in Silicon Nitride," *J. Am. Ceram. Soc.*, **78** [9] 2345–52 (1995).

[49]J. Selsing, "Internal Stresses in Ceramics," *J. Am. Ceram. Soc.*, **44** [8] 419 (1961).

[50]P. Andrews and F. L. Riley, "Silicon Nitride Oxidation/Re-Oxidation," *J. Eur. Ceram. Soc.*, **7**, 125–32 (1991).

[51]D. R. Clarke and F. F. Lange, "Oxidation of Silicon Nitride Alloys: Relation to Phase Equilibria in the System Si_3N_4–SiO_2–MgO," *J. Am. Ceram. Soc.*, **63** [9–10] 586–93 (1980).

[52]M. Backhaus-Ricoult and Y. G. Gogotsi, "Identification of Oxidation Mechanisms in Silicon Nitride Ceramics by Transition Electron Microscopy Studies of Oxide Scales," *J. Mater. Res.*, **10** [9] 2306–21 (1995).

[53]G. Nickel, R. Danzer, G. Schneider, and G. Petzow, "Corrosion and Oxidation of Advanced Ceramics," *Powder Met. Int.*, **21** [3] 29–33 (1989).

[54]R. O. Jones and O. Gunnarsson, "The Density Functional Formalism, its Applications and Prospects," *Rev. Mod. Phys.*, **61** [7] 721–46 (1989).

[55]R. S. Aujla, G. Leng-Ward, M. H. Lewis, E. F. W. Seymour, G. A. Styles, and G. W. West, "An NMR Study of Silicon Coordination in Y–Si–Al–O–N Glasses," *Philos. Mag., B*, **54** [8] L51–6 (1986).

[56]R. K. Sato, J. Bolvin, and P. F. McMillan, "Synthesis and Characterization of a SiAlON Glass," *J. Am. Ceram. Soc.*, **73** [8] 2494–7 (1990).

[57]R. E. Loehman, "Preparation and Properties of Yttrium–Silicon–Aluminum Oxynitride Glasses," *J. Am. Ceram. Soc.*, **62** [9–10] 491–4 (1979).

[58]M. J. Hoffmann, A. Geyer, and R. Oberacker, "Potential of the Sinter-HIP-Technique for the Development of High-Temperature Resistant Si_3N_4–Ceramics," *J. Eur. Ceram. Soc.*, **19**, 2359–66 (1999).

[59]G. N. Babini, A. Bellosi, and P. Vincenzini, "A Diffusion Model for the Oxidation of Hot-Pressed Si_3N_4–Y_2O_3–SiO_2 Materials," *J. Mater. Sci.*, **19**, 1029–42 (1984).

[60]D. Cubicciotti and K. H. Lau, "Kinetics of Oxidation of Hot-Pressed Silicon Nitride Containing Magnesia," *J. Am. Ceram. Soc.*, **61** [11–12] 512–7 (1978).

[61]D. Cubicciotti and K. H. Lau, "Kinetics of Oxidation of Yttria Hot-Pressed Silicon Nitride," *J. Electrochem. Soc.*, **126** [10] 1723–8 (1979).

[62]D. Cubicciotti, K. H. Lau, and R. L. Jones, "The Rate Controlling Process in the Oxidation of Hot Pressed Silicon Nitride," *J. Electrochem. Soc.*, **124** [12] 1955–6 (1977).

[63]J. Echeberria and F. Castro, "Oxidation of Silicon Nitride Sintered with Ceria and Alumina," *Mater. Sci. Tech.*, **6** [6] 497–503 (1990).

[64]Y. G. Gogotsi, G. Grathwohl, F. Thümmler, V. P. Yaroshenko, M. Herrmann, and C. Taut, "Oxidation of Yttria- and Alumina-Containing Dense Silicon Nitride Ceramics," *J. Eur. Ceram. Soc.*, **11**, 375–86 (1993).

[65]A. Geyer "Potential des Sinter-HIP-Verfahrens in der Entwicklung von Siliziumnitridwerkstoffen für den Hochtemperaturbereich," Ph.D. Thesis, University of Karlsruhe, Germany, 1998.

[66]T. Nakayasu, T. Yamada, I. Tanaka, H. Adachi, and S. Goto, "Calculation of Grain-Boundary Bonding in Rare-Earth-Doped β-Si_3N_4," *J. Am. Ceram. Soc.*, **81** [3] 565–70 (1998).

[67]P. Dudesek and L'. Benco, "Cation-Aided Joining of Surfaces of ß-Silicon Nitride: Structural and Electronic Aspects," *J. Am. Ceram. Soc.*, **81** [5] 1248–54 (1998).

[68]L'. Benco, "Chemical Bonding at Grain Boundaries: MgO on ß-Si_3N_4," *Surface Sci.*, **327**, 274–84 (1995).

[69]A. Ziegler, C. Kisielowski, M. J. Hoffmann, and R. O. Ritchie, "Atomic Resolution Transmission Electron Microscopy of the Intergranular Structure of a Y_2O_3-Containing Silicon Nitride Ceramic," *J. Am. Ceram. Soc.*, **86** [10] 1777–85 (2003).

[70]M. Yoshiya, K. Tatsumi, I. Tanaka, and H. Adachi, "Theoretical Study on the Chemistry of Intergranular Glassy Film in Si_3N_4–SiO_2 Ceramics," *J. Am. Ceram. Soc.*, **85** [1] 109–12 (2002).

[71]S. H. Garofalini and W. Luo, "Molecular Dynamics Simulations of Calcium Silicate Intergranular Films between Silicon Nitride Crystals," *J. Am. Ceram. Soc.*, **86** [10] 1741–52 (2003).

[72]N. Shibata, S. J. Pennycook, T. R. Gosnell, G. S. Painter, W. A. Shelton, and P. F. Becher, "Observation of Rare-Earth Segregation in Silicon Nitride Ceramics at Subnanometre Dimensions," *Nature*, **428**, 730–3 (2004). □